A Self-Referencing Method for Microplate Label-Free Photonic-Crystal Biosensors

Leo L. Chan, Brian T. Cunningham, *Member, IEEE*, Peter Y. Li, and Derek Puff

***Abstract*—To improve the accuracy of optical biosensors, a reference sensor is often incorporated in close proximity to the sensor performing the detection function in order to compensate for common-mode error sources that result in a detected signal but are not a result of biochemical binding to the sensor surface. These error sources include thermal drift, the refractive index of the test sample, and nonspecific binding. Because photonic-crystal biosensors do not allow lateral propagation of light along their surface, spatial images of biochemical-binding density may be generated in which each individual pixel of the image represents an independent sensor. Using this capability, a small region of a photonic-crystal surface can effectively contain a large number of "active" and "reference" pixels when the immobilized ligand is applied to only a portion of the imaged region. In this paper, the use of a photonic-crystal optical biosensor assay protocol and data-analysis method that results in elimination of common-mode error sources from the detected signal is described. When applied to biosensors embedded within a standard 96-well microplate format, the new method enables the use of nanoliter-scale quantities of immobilized ligand reagent, is insensitive to immobilized ligand nonuniformity, and allows rapid analysis of many biochemical assays in parallel.**

***Index Terms*—Biosensor, label free, pharmaceutical, self-referencing.**

I. Introduction

A FUNDAMENTAL aspect of many types of optical biosensors is the generation of signals that are not due to the quantity of interest but rather due to some other type of input to the sensor system. For label-free detection of small molecules or for detection of larger molecules at exceedingly low concentrations, the detected signal is often so small that it is of similar magnitude to the noise introduced by the experiment [1]. In order to extract a meaningful signal in these cases, it is critical to be able to accurately separate the signal caused by experimental artifacts from the biochemical-binding signal. Noise sources that have the capability for changing sensor response are the bulk refractive index of the test sample and nonspecific adsorption of unwanted biomolecules to the sensor surface. Such common-mode errors are typically corrected through the use of a "reference" sensor that is monitored in parallel with the "active" sensor. In the context of biosensors integrated with microfluidic channels, the reference sensor may be exposed to a separately controlled flow stream than the active sensor, so that the receptor ligand is deposited only on the active sensor, but both the active and reference sensors are exposed to the test sample simultaneously [2], [3]. In the context of biosensors embedded within 96- or 384-well multiwell microplates, individual wells may be designated as references, and the position and number of reference wells are selected based upon the accuracy required for a particular assay and the expected variability in common-mode error effects [4].

In previous work, we have described a novel biosensor technology based upon photonic crystals [5]. The sensor utilizes a subwavelength periodic surface structure that, when illuminated with white light at normal incidence, reflects only a very narrow (resonant) band of wavelengths [6]–[8]. The resonant peak wavelength value (PWV) is modified by the attachment of biomolecules, so that small changes in surface dielectric permittivity can be quantified without an attachment of a label to the detected biomolecule. The sensor structure is mass manufactured from continuous sheets of plastic film and incorporated into single-use disposable labware such as 96-, 384-, or 1536-well microplates for high-throughput assay applications in pharmaceutical discovery and life science research [9]. With an appropriate detection instrument, the density of biochemical binding on the sensor surface can be measured in a high spatial-resolution-imaging mode in which an entire microplate surface may be scanned [10]. With the sensor structure illuminated at normal incidence by a collimated beam, only a zeroth-order resonant coupling occurs. A photonic band gap is designed in the direction of periodicity (lateral to the surface) that cuts off the propagation of modes parallel to the surface. The zeroth-order coupling allows the sensor resonance to be detected as a mirror image of the surface, while the lack of lateral propagation ensures no optical crosstalk between adjacent sensor regions.

Because the photonic-crystal biosensor measures the changes in dielectric permittivity on the sensor surface, the addition of material to the sensor that results in a change of the refractive index of the liquid media in contact with the sensor will induce a signal that is indistinguishable from an actual biochemical-binding event [1], [11]. Small molecule analytes are often suspended in solutions that are partly comprised of solvents, such as Dimethyl Sulphoxide (DMSO) [12], glycerol, and ethanol, to prevent precipitation. The solvents have a refractive index, which is different from that of water or buffer solution, and therefore, the variability of solvent content from one sample to another within a chemical library results in a measurement

Manuscript received December 12, 2005; revised March 8, 2006 and March 30, 2006. This material is based on work supported by the National Science Foundation under Grant 0427657. This work was supported by SRU Biosystems. The associate editor coordinating the review of this paper and approving it for publication was Dr. Jenny Gun.

L. L. Chan and B. T. Cunningham are with the Nano Sensors Group, Micro and Nanotechnology Laboratory, University of Illinois at Urbana–Champaign, Urbana, IL 61801 USA (e-mail: Lchan1@uiuc.edu; bcunning@uiuc.edu).

P. Y. Li and D. Puff are with SRU Biosystems, Woburn, MA 01801 USA (e-mail: info@srubiosystems.com).

Color versions of Figs. 1–4 are available at http://ieeexplore.ieee.org.

Digital Object Identifier 10.1109/JSEN.2006.884547

variability for optical biosensors that is due solely to the refractive index of the test sample.

In this paper, we demonstrate a method for highly accurate compensation of bulk refractive-index errors by an integration of active and reference regions of the photonic-crystal biosensor within each biosensor microplate well. The method requires the application of the immobilized ligand to only a portion of the biosensor well, so the active and reference regions of the biosensor surface can be exposed to the same analyte test sample. Using the high spatial-resolution-imaging capabilities of the biosensor detection instrument, hundreds of independent biosensor measurements are gathered simultaneously for each well to rapidly construct a plot for detected analyte concentration as a function of immobilized ligand density, where reference regions of the sensor have an immobilized ligand density of zero. The slope of this plot is used to quantify the detection of analyte, while the y-intercept contains information about error effects that occur to the "active" and "reference" regions in common. This approach is insensitive to the exact location, size, uniformity, and shape of the immobilized ligand region, and it reduces the complex image analysis to a single number (slope of plot) for each biosensor microplate well.

II. Materials and Methods

A. Sensors and Instrument

The design and fabrication of the photonic-crystal sensors used in this paper have been published previously [11], [13]. The other sensor, when illuminated with a broadband light source, reflects only a narrow resonant band of wavelengths. Shifts in the reflected PWV are measured due to attachment of material to the sensor surface. The sensors used in the work presented here were incorporated into standard 96-well microplates. The biosensor imaging instrument has also been described previously [10], [14]. The instrument measures the biosensor resonant reflected PWV as a function of position on the biosensor surface in order to generate a PWV image of the entire sensor surface in a single scan. A pixel resolution of 89.2×89.2 μm^2 was used in this paper, and the time required to scan a plate is $\sim$600 s.

Typically, a biosensor experiment involves measuring shifts in PWV, so the sensor surface is scanned twice—once before and once after the biomolecular binding—and the images are aligned and subtracted to determine the difference in PWV as detected by the sensor. This scanning method does not require the PWV of the imaged surface to be completely uniform, either across the surface or within a set of probe locations, or tuning of the sensor angle to have a resonance condition, as with surface-plasmon-resonance imaging [15].

B. Effect of Bulk Refractive Index on Biosensor Signal

Bulk refractive-index-induced PWV shifts were intentionally induced by the introduction of the solvent DMSO to a buffer solution. The DMSO was mixed with 0.01-M phosphate buffered saline (PBS, pH $= 7.4$; Sigma–Aldrich) to produce 21 different DMSO concentrations ranging from 0% to 2% in increments of 0.1%. To measure the effect of DMSO concentration on the biosensor PWV, the sensor PWV was initially measured with 50 μL of PBS solution. Next, the PBS solution was replaced by the DMSO/PBS mixtures with one DMSO concentration per well and four replicate wells per concentration. After signal stabilization, the biosensor PWVs were measured a second time.

C. Protein A–Immunoglobulin-G (IgG) Assay

A protein–protein bioassay was performed that compares the binding affinity between Protein A and IgG from five different animals in the presence of intentionally introduced DMSO bulk refractive-index errors. Protein A (Pierce Biotechnology) was prepared with 0.01-M PBS and filtered with a 0.22-μm syringe filter (Nalgene) to a concentration of 0.1 mg/ml. The five IgGs are from rabbit, sheep, goat, rat, and chicken, each diluted in 0.01-M PBS to a concentration of 0.5 mg/ml. Six DMSO concentrations (0.4%, 0.7%, 1.0%, 1.3%, 1.6%, and 2.0%) were introduced along with the IgG buffer solutions.

The 96 wells on the microplate were incubated with 100 μL of PBS for 30 min on a rotator (LAB-LINE), and the top of the microplate was sealed with a thermal seal (Fisher Scientific) to prevent evaporation of the buffer solution. After the surface was stabilized, the microplate was scanned (SCAN A), and then, the PBS was removed from each well, and the surface was completely dried with pressurized N_2. Each well was then spotted with one 4.0-nL spot of Protein A by a multispot dispenser (Piezoarray; Perkin Elmer, Inc.) near the center of the well and allowed to adsorb to the sensor surface and dry for more than 30 min. For simplicity, the Protein A was attached directly to the TiO_2 surface of the sensor by adsorption without the use of covalent surface chemistry or bifunctional linkers.

Next, the wells were rinsed three times with PBS to wash away loosely bounded Protein A on the surface and filled with 100 μL of PBS for the second scan (SCAN B). Experiments (not shown) with identical sensors using a detection instrument with kinetic measurement capabilities were used to verify the adsorbed Protein A layer, which is stably attached and does not undergo dissociation during IgG binding steps. Undiluted Seablock solution (Pierce Biotechnology) was added to each well at a volume of 100 μL without removing the PBS solution, and allowed to incubate for 50 min. The Seablock/PBS solution was removed, and the wells were washed five times with PBS, and a final volume of 100 μL was incubated for a postblocking scan (SCAN C). The PBS solution was replaced with 90 μL of 0.0%, 0.4%, 0.7%, 1.0%, 1.3%, 1.6%, and 2.0% DMSO solution in columns 1, 2–3, 4–5, 6–7, 8–9, 10–11, and 12, respectively. The DMSO solutions were allowed to incubate for 30 min before the addition of the 0.5-mg/ml IgG solutions, where 10 μL of rabbit, sheep, goat, rat, chicken IgG, and PBS were pipetted into rows C, D, E, F, G, and H, respectively. The analyte was allowed to incubate for 50 min before the microplate was scanned for the fourth time (SCAN D). The sequence of steps is summarized in Fig. 1.

D. Self-Referencing Data Analysis

The first scan [scan "A" in Fig. 1(a)] establishes the preassay baseline PWV image for the chemically functionalized plate

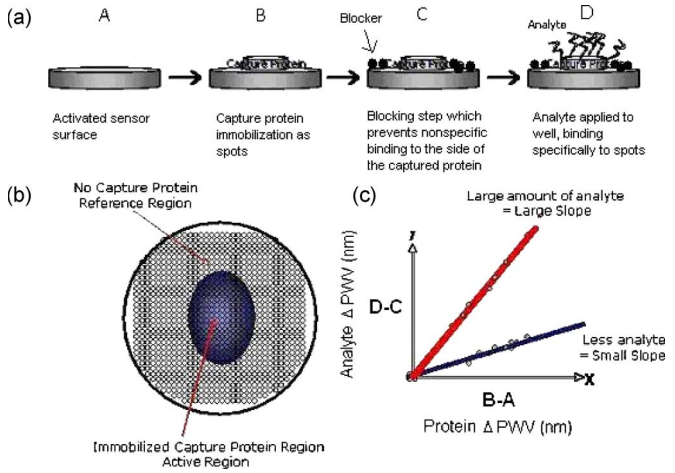

Fig. 1. Schematic representation of the slope method for self-referenced label-free binding analysis. (a) Sequence of four scans required to determine the spatial density of immobilized protein (Scan B–Scan A) and the density of the detected analyte (Scan D–Scan C). (b) Representation of a single biosensor microplate well, subdivided into a grid of independent PWV determinations from an array of pixels. Pixels without captive protein function as reference measurements for correction of common-mode errors for pixels within the active regions with immobilized protein. (c) Plot of immobilized protein density (x-axis) versus the detected analyte density (y-axis) yields a linear plot, whose slope indicates the relative affinity between analyte and ligand.

immediately before the protein ligand is applied. The second scan [scan "B" in Fig. 1(a)] measures the PWV image after the protein-ligand spot is applied and after any unbound protein has been washed away. By mathematically subtracting the PWV image of scan "A" from the PWV image of scan "B," we obtain a PWV shift image that displays the immobilized protein density as a function of position in each well of the microplate. The third scan [scan "C" in Fig. 1(a)] measures the PWV image after a blocker is introduced into the well to prevent nonspecific binding of analytes on the sensor surface. The final scan [scan "D" in Fig. 1(a)] measures the PWV image of the microplate after exposure to the analyte. By mathematically subtracting the PWV image of scan "C" from the PWV image of scan "D," we obtain a PWV shift image that displays the detected analyte density as a function of position in each well of the microplate.

As shown in Fig. 1(c), the data gathered from the four scans can be used to generate a plot of the detected analyte density as a function of immobilized protein density, where each individual pixel from the PWV shift image represents one point (pixel) from the protein density continuum generated by the immobilized protein spot. The range of PWV was selected to include every "reference" pixel and every "active" pixel in the generated plot. Because the detected analyte density is linearly dependent upon the availability of immobilized protein on the sensor surface, a linear trend is measured. The slope of this linear trend serves as a means of quantifying the strength of the interaction between the immobilized protein and the analyte: Greater slope indicates greater interaction strength than lesser slope, and zero indicates no interaction. Since a greater binding affinity produces higher PWV shifts from the analytes, greater affinity increases the vertical value of the active pixels, thus increasing the slope of the plot. An important consequence of this data-analysis method is that the bulk refractive index of the analyte solution has no effect on the slope of the plot,

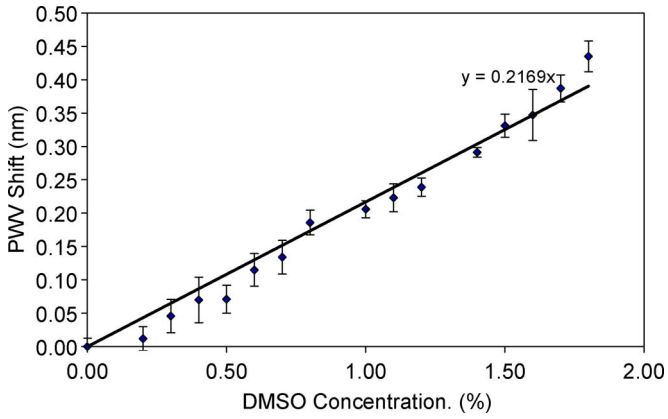

Fig. 2. PWV shift of the biosensor as a function of the DMSO concentration in PBS buffer.

although it can change the y-intercept of the curve. Because, the bulk refractive index of the buffer solution will change the PWVs collected for each pixel, thus moving all of the data points along the y-axis. In this way, the regions of the microplates that do not contain the immobilized protein serve as a reference for correcting the effect of bulk refractive index in the analyte sample. Although the data-analysis method is based upon the high-resolution images of biochemical-binding density, the image analysis is reduced to the reporting of a single number, which is the slope of the immobilized ligand density/analyte density curve that can be utilized as a means for screening higher affinity binders from lower affinity binders.

III. Results

A. DMSO Bulk Refractive-Index Calibration

Fig. 2 plots the bulk PWV shift as a function of DMSO concentration in buffer solution. A linear trend of the PWV shift versus the DMSO concentration is observed as expected, with a bulk shift coefficient $(\Delta\lambda/\Delta\mathrm{DMSO}\%)$ of 0.22 nm/%. Thus, if the minimum resolvable PWV shift is $\Delta\mathrm{PWV}(\mathrm{min}) = 0.001$ nm, then a DMSO-concentration variability of $\sim$0.005% between two samples would generate a measurable error.

B. Protein A—IgG Affinity With DMSO Solution Error

The measured Protein A PWV shift was uniform across the microplate at $\sim 0.35 \pm 0.05$ nm. Fig. 3 shows the PWV images for a single well of the microplate, where the 4-nL Protein A dispensed volume results in a $\sim 340 \times 460$-μm^2 spot area with a maximum PWV shift $\sim$0.40 nm. Fig. 3(a) shows the PWV shift image for immobilized Protein A (SCAN B–SCAN A), while Fig. 3(b) shows the PWV shift due to a selective attachment of rabbit IgG to the Protein A. The blocking protocol was effective for preventing adsorption of IgG to the region of the sensor surface without Protein A. Fig. 4 shows a sample plot of detected IgG (y-axis) as a function of immobilized Protein A PWV shift (x-axis). Because the immobilized spots are small compared to the microplate well, most accurate referencing is obtained by only considering a ~ 500-μm diameter circular region immediately surrounding the spot for the analysis. Regions as large as the entire microplate well may be included if desired.

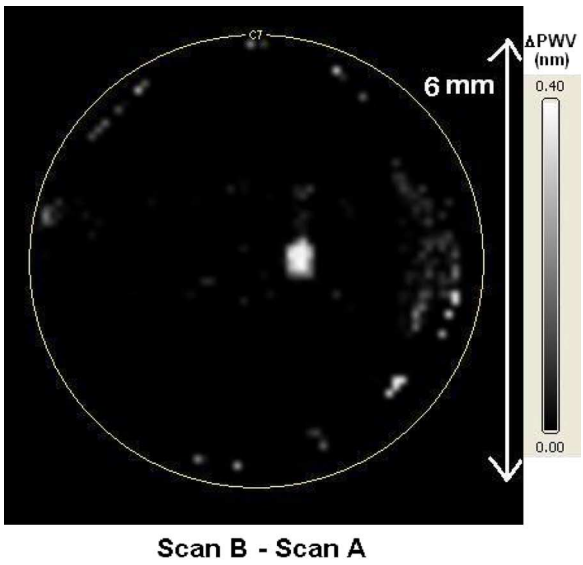

(a)

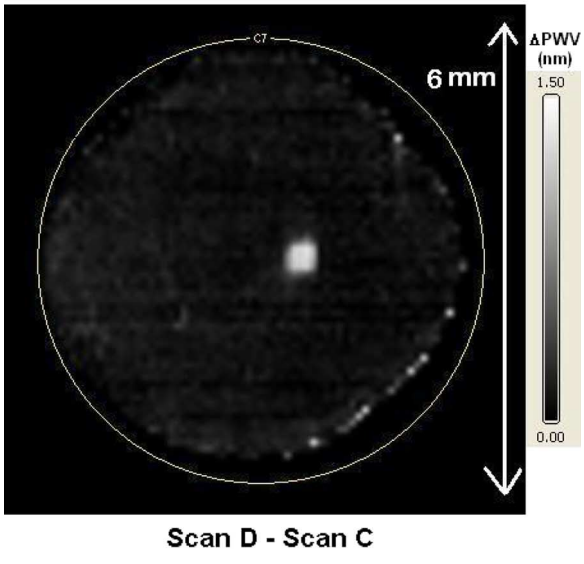

(b)

Fig. 3. PWV shift images for a single microplate well scanned at a pixel resolution of $89.2 \times 89.2\ \mu\text{m}^2$. (a) PWV shift image (Scan B–Scan A) of a single spot of immobilized Protein A applied with a volume of 4 nL. (b) PWV shift image (Scan D–Scan C) for analyte rabbit IgG binding to the immobilized Protein A spot.

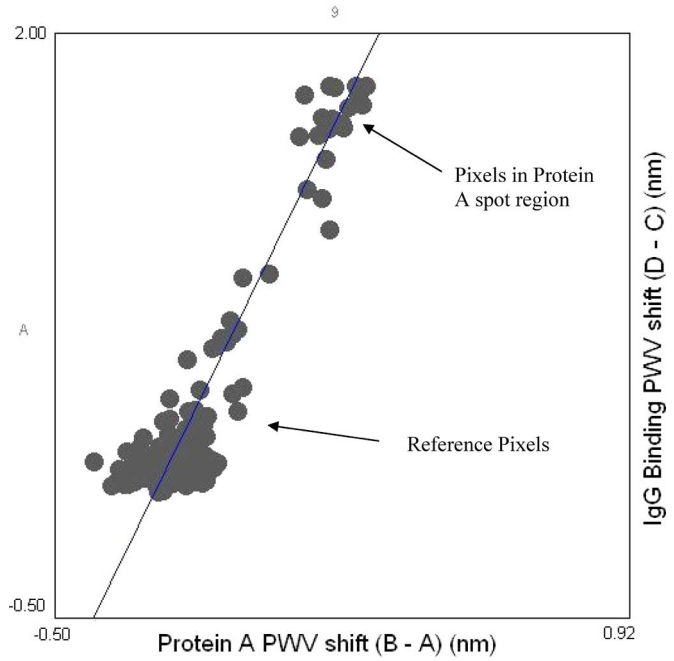

Fig. 4. Sample scatter plot of rabbit IgG binding density as a function of immobilized Protein A density for a single well of the biosensor microplate. Each point in the plot represents a single pixel from the PWV image. Therefore, points near the origin represent pixels with no immobilized Protein A (reference), while points away from the origin represent pixels with immobilized Protein A (active).

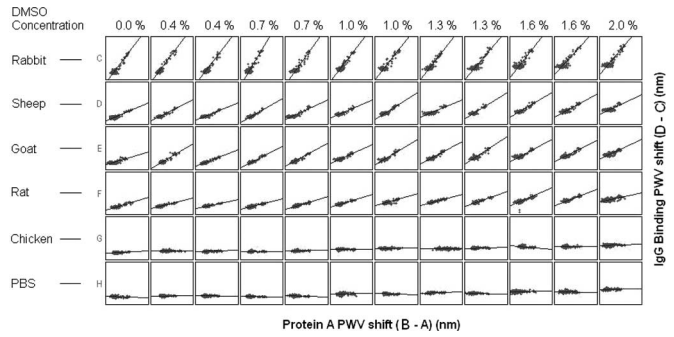

Fig. 5. Scatter plots with best fit lines for 72 biosensor microplate wells. Each well contains a single immobilized Protein A spot and is exposed to a single IgG at 0.05-mg/ml concentration in the presence of variable concentrations of DMSO. For each scatter plot, the Protein A binding density (Scan B–Scan A) is plotted on the x-axis, and the ligand binding density (Scan D–Scan C) is plotted on the y-axis.

Note that each point in the scatter plot corresponds to a single pixel of the PWV image.

Best fit lines were generated with the pixels obtained from each microplate well with a least square fit algorithm. The slope and y-intercept were determined from the fitted line. The scatter plots with best fit lines for each microplate well are shown in Fig. 5, where greater slope indicates greater binding of the IgG to the immobilized Protein A spot. Due to nonuniformity in the density of the immobilized Protein A spot, the x-axis does not register an identical PWV shift for each pixel.

The measured slope values shown in Fig. 6 correlate with the expected binding affinity of each animal IgG, where the rabbit IgG has high binding affinity, sheep, goat, and rat IgG have low binding affinity, and chicken IgG has no binding affinity [16]. The intercept values for each microplate well are shown in Fig. 7. Note that as the concentration of DMSO increases, the y-intercept values increase, as expected.

IV. Discussion and Conclusion

The images of the Protein A spots showed binding to the sensor surface with no noticeable spreading effects, even after washing with PBS [Fig. 3(a)]. The Protein A is strongly adsorbed on to the sensor surface; even with a strong PBS washing cycle, only a small amount of Protein A would wash off, which is compensated by the mathematical subtraction of Scan B–Scan A. Furthermore, the blocking step with undiluted Seablock effectively prevented a nonspecific binding to the sensor surface and allowed the IgGs to bind only to the area with Protein A. The scatter plots from the microplate wells showed

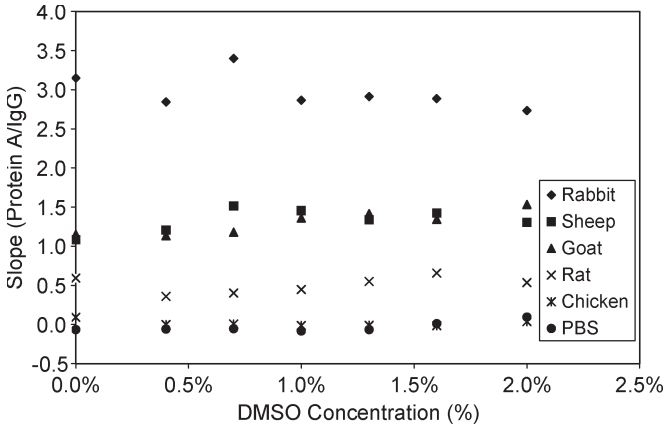

Fig. 6. Slope value as a function of the DMSO concentration for each animal IgG. The determined slope is greatest for Protein A-IgG interactions with greatest affinity and is not dependent upon the DMSO concentration.

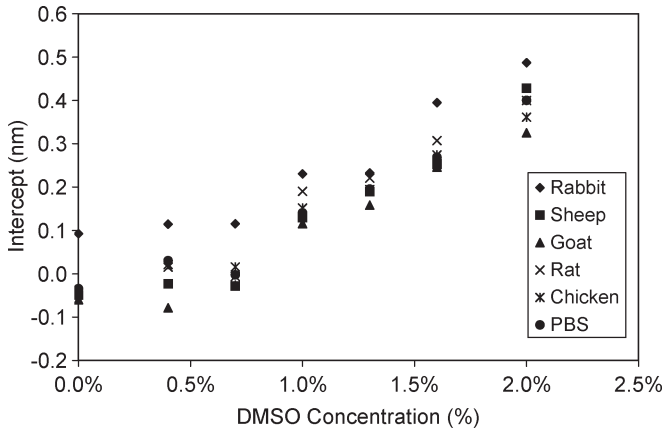

Fig. 7. y-intercept values as a function of the DMSO concentration for each animal IgG. The relationship between the DMSO concentration and y-intercept values contains information on assay artifacts that affect both the reference and active regions of the well.

two clusters of pixels. The cluster near the origin represents the reference pixels, whereas the active pixels are in the cluster away from the origin shown in Fig. 4. The intercept of the plots represents the bulk PWV shift due to the addition of different DMSO concentrations to the buffer solution in the microplate wells. Fig. 7 plots the bulk PWV shift for each concentration of DMSO and for each animal IgG. The intercept values increase as the DMSO concentration increases, because every pixel in the (Scan D–Scan C) image is equally affected by the bulk refractive-index shift. For all of the IgGs with the exception of rabbit IgG, the 0.0% DMSO condition resulted in a slightly negative y-intercept, which is presumed to be the result of a small negative PWV drift between Scan C and Scan D. Such drift, if occurring on the entire biosensor microplate in common, is also factored out of the slope analysis. The highest affinity IgG in the panel (rabbit) exhibited a measurable nonspecific binding to the reference regions of the well, as shown by the positive value for y-intercept with 0.0% DMSO in Fig. 7. Due to the experimental artifacts, such as surface wetting during spot application and spot drying during incubation, it is difficult to achieve the immobilized spots with perfectly uniform density. Instead, one obtains a continuum of immobilized Protein A density ranging from zero to a maximum value, as determined by the Scan B–Scan A measurement. For a saturating analyte concentration, the analyte signal will be linearly dependent upon the immobilized ligand concentration. As long as the linear relationship holds, we measure a linear slope in the plots that measure the immobilized ligand density (Scan B–Scan A) as a function of detected analyte density (Scan D–Scan C). If the immobilized protein orientation or activity varied as a function of immobilized protein density, these factors could cause our plot to become nonlinear.

Fig. 6 shows that for analytes stored in 1%–2% DMSO buffers, DMSO-concentration variability as great as 100% from one sample to another will have a little impact upon the actual binding signal as measured by the slope. Because the actual DMSO variability is expected to be no more than 10% in a protein affinity screening campaign, the determination of binding affinity by the "slope method" is effective for elimination of bulk refractive-index errors.

The self-referencing assay protocol and image-analysis technique presented here is enabled by the ability to gather high-resolution spatial images of label-free biomolecular binding on the biosensor surface. The assay method described in this paper requires only a few nanoliters of immobilized protein solution per well, resulting in the use of only $\sim$28.8 ng of protein per assay. This is particularly important for assays requiring expensive purified protein that is available in small quantity but which must be used in a screening campaign involving thousands of wells.

The image-analysis method does not require the immobilized protein spot to be deposited in any particular location within the biosensor microplate well and does not require the spot to be deposited with any particular shape. In fact, the slope-analysis method does not require absolutely uniform immobilized protein density, provided that the activity of the protein is uniform. Although four sequential scans of the microplate are required, each scan takes $\sim$10 min. The image alignment, subtraction, and slope determination functions are automated by the detection instrument software. The scan time can be substantially reduced by decreasing the pixel resolution or by limiting the data collection only to regions of the microplate wells of greatest interest. Future work on the self-referencing slope method will involve experimenting with small-molecule detection and low-concentration protein-analyte binding.

ACKNOWLEDGMENT

The authors would like to thank X. Li and the support staff of the University of Illinois Metabolomics Center for the use of Perkin–Elmer Piezoarray. Any opinions, findings, and conclusions or recommendations expressed in this material are those of the author(s) and do not necessarily reflect the views of the National Science Foundation.

REFERENCES

[1] B. Lin, J. Pepper, P. Li, H. Pien, and B. T. Cunningham, "A label-free high throughput optical technique for detecting small molecule interactions," *Biosens. Bioelectron.*, vol. 17, no. 9, pp. 827–834, Sep. 2002.

[2] B. Liedberg, C. Nylander, and I. Lundstrom, "Surface plasmon resonance for gas detection and biosensing," *Sens. Actuators*, vol. 4, no. 2, pp. 299–304, 1983.

[3] E. A. Smith and R. M. Corn, "SPR imaging as a tool to monitor biomolecular interactions in an array based format," *Appl. Spectrosc.*, vol. 57, no. 11, pp. 320A–332A, 2003.
[4] C. E. Jordan and R. M. Corn, "Surface plasmon resonance imaging measurements of electrostatic biopolymer adsorption onto chemically modified gold surfaces," *Anal. Chem.*, vol. 69, no. 7, pp. 1449–1456, 1997.
[5] B. T. Cunningham, P. Li, B. Lin, and J. Pepper, "Colorimetric resonant reflection as a direct biochemical assay technique," *Sens. Actuators B, Chem.*, vol. 81, no. 2/3, pp. 316–328, Jan. 2002.
[6] S. S. Wang and R. Magnusson, "Theory and applications of guided-mode resonance filters," *Appl. Opt.*, vol. 32, no. 14, pp. 2606–2613, May 1993.
[7] ——, "Design of waveguide-grating filters with symmetrical line shapes and low sidebands," *Opt. Lett.*, vol. 19, no. 12, pp. 919–921, Jun. 1994.
[8] R. Magnusson and S. S. Wang, "New principle for optical filters," *Appl. Phys. Lett.*, vol. 61, no. 9, pp. 1022–1024, Aug. 1992.
[9] B. T. Cunningham, P. Li, S. Schulz, B. Lin, C. Baird, J. Gerstenmaier, C. Genick, F. Wang, E. Fine, and L. Laing, "Label-free assays on the BIND system," *J. Biomol. Screen.*, vol. 9, no. 6, pp. 481–490, 2004.
[10] P. Li, B. Lin, J. Gerstenmaier, and B. T. Cunningham, "A new method for label-free imaging of biomolecular interactions," *Sens. Actuators B, Chem.*, vol. 99, no. 1, pp. 6–13, Apr. 2004.
[11] B. T. Cunningham, J. Qiu, P. Li, and C. Baird, "Enhancing the surface sensitivity of colorimetric resonant optical biosensors," *Sens. Actuators B, Chem.*, vol. 87, no. 2, pp. 365–370, Dec. 2002.
[12] H. J. Lee, G. Shan, T. Watanabe, D. W. Stoutamire, S. J. Gee, and B. D. Hammock, "Enzyme-linked immunosorbent assay for the pyrethroid deltamethrin," *J. Agric. Food Chem.*, vol. 50, no. 20, pp. 5526–5532, 2002.
[13] B. T. Cunningham, J. Qiu, P. Li, J. Pepper, and B. Hugh, "A plastic colorimetric resonant optical biosensor for multiparallel detection of label-free biochemical interactions," *Sens. Actuators B, Chem.*, vol. 85, no. 3, pp. 219–226, Jul. 2002.
[14] B. Lin, P. Li, and B. T. Cunningham, "A label-free biosensor-based cell attachment assay for characterization of cell surface molecules," *Sens. Actuators B, Chem.*, vol. 114, no. 2, pp. 559–564, Apr. 2005.
[15] E. A. Smith, W. D. Thomas, L. L. Kiessling, and R. M. Corn, "Surface plasmon resonance imaging studies of protein-carbohydrate interactions," *J. Amer. Chem. Soc.*, vol. 125, no. 20, pp. 6140–6148, 2003.
[16] D. D. Richman, P. H. Cleveland, M. N. Oxman, and K. M. Johnson, "The binding of Staphylococci protein a by the sera of different animal species," *J. Immunol.*, vol. 128, no. 5, pp. 2300–2305, May 1982.

Leo L. Chan received the B.S. and M.S. degrees in electrical and computer engineering with a minor in biomedical engineering from University of Illinois at Urbana–Champaign, Urbana, where he is currently working toward the Ph.D. degree.

He is a Graduate Research Assistant with University of Illinois at Urbana–Champaign in the Nano Sensors Group directed by Dr. B. T. Cunningham. His research focuses on the characterization of photonic-crystal optical biosensors and the optimization of small molecule biodetection using this platform. Before joining Dr. Cunningham's group, he served as an Undergraduate Researcher with Keck Graduate Institute, Claremont, CA, where he worked on the application of free solution electrophoresis to DNA finger printing.

Brian T. Cunningham (M'02) received the B.S., M.S., and Ph.D. degrees in electrical and computer engineering from University of Illinois at Urbana–Champaign, Urbana. His thesis research was in the field of optoelectronics and compound semiconductor material science, where he contributed to the development of crystal growth techniques that are now widely used for manufacturing solid state lasers, and high-frequency amplifiers for wireless communication.

He is an Associate Professor of electrical and computer engineering with University of Illinois at Urbana–Champaign, where he is the Director of the Nano Sensors Group. His group focuses on the development of photonic-crystal-based transducers, plastic-based fabrication methods, and novel instrumentation approaches for label-free biodetection. He is a Founder and the Chief Technical Officer of SRU Biosystems, Woburn, MA: a life science tools company that provides high-sensitivity plastic-based optical biosensors, instrumentation, and software to the pharmaceutical, academic research, genomics, and proteomics communities. Prior to founding SRU Biosystems in June 2000, he was the Manager of biomedical technology with Draper Laboratory, Cambridge, MA, where he directed R&D projects aimed at utilizing defense-related technical capabilities for medical applications. In addition, he served as a Group Leader for MEMS Sensors with Draper Laboratory, where he directed a group performing applied research on microfabricated inertial sensors, acoustic sensors, optical switches, microfluidics, tissue engineering, and biosensors. Concurrently, he was an Associate Director with the Center for Innovative Minimally Invasive Therapy (CIMIT)—a Boston-area medical technology consortium—where he led the Advanced Technology Team on Microsensors. Before working with Draper Laboratory, he spent five years with the Raytheon Electronic Systems Division, developing advanced infrared imaging array technology for defense and commercial applications.

Peter Y. Li received the Ph.D. degree in physics from Purdue University, West Lafayette, IN.

He has been a Postdoctoral Fellow with the University of Minnesota. He is currently the Director of Product Development with SRU Biosystems, Woburn, MA, which is a life science tools company that provides high-sensitivity plastic-based optical biosensors, instrumentation, and software to the pharmaceutical, academic research, genomics, and proteomics communities. Prior to joining SRU Biosystems, he worked in the field of medical imaging systems with Eastman Kodak Company, Imation Corp., and 3M Company. He has authored 13 issued U.S. patents and numerous scientific journal articles. His research and development interests include imaging systems, optical systems, and scientific instrumentation. During his academic career, his research has focused on surface physics, specializing in scanning tunneling microscopy studies of metals and semiconductors.

Derek Puff received the Ph.D. degree in biomedical engineering from the University of North Carolina, Chapel Hill, in 1995, where he specialized in medical image processing and analysis.

He is the Principal Software Engineer with SRU Biosystems, Inc., Woburn, MA: a biotechnology firm developing high-sensitivity biosensors for label-free molecular interaction detection. He has worked as a Software Developer with the medical imaging and biotechnology industry for the past ten years. He leads the development of software applications for the SRU Biosystems instrumentation product line.